Synthesis and attachment of silver and copper nanoparticles on cellulose nanofibers and comparative antibacterial study

Duy-Nam Phan · Nasanjargal Dorjjugder · Muhammad Qamar Khan · Yusuke Saito · Goro Taguchi · Hoik Lee · Yasuhito Mukai · Ick-Soo Kim

Abstract Metal nanoparticles are considered intriguing to academic society, due to a wide spectrum of applications in electronics, biomedical engineering, optics, and medicine. In this study, effective methods of decorating cellulose nanofibers (CNFs), deacetylated from cellulose acetate nanofibers, with silver nanoparticles (AgNPs) via ultraviolet radiation and copper nanoparticles (CuNPs) via chemical reduction were reported. The formation of metal nanoparticles was confirmed by scanning electron microscopy and transmission electron microscopy. The sizes and the metal contents of AgNPs incorporated CNFs (Ag/CNFs) were demonstrated to correlate well with the concentrations of immersion solutions; whereas sizes of CuNPs decorated CNFs, denoted as Cu/CNFs, did not change significantly upon the increased concentrations of wetting solutions. Bacterial inhibition zones and the bactericidal efficacy were investigated against both gram-negative and gram-positive bacteria; interestingly, the results revealed superior bactericidal activity against *E. coli* for Ag/CNFs and better antibacterial properties against *B. subtilis* for Cu/CNFs.

D.-N. Phan · Y. Saito · I.-S. Kim (✉)
Nano Fusion Technology Research Group, Division of Frontier Fibers, Institute for Fiber Engineering (IFES), Interdisciplinary Cluster for Cutting Edge Research (ICCER), Shinshu University, Tokida 3-15-1, Ueda, Nagano 386-8567, Japan
e-mail: kim@shinshu-u.ac.jp

N. Dorjjugder · G. Taguchi
Gene Research Center, Shinshu University, Tokida 3-15-1, Ueda, Nagano 386-8567, Japan

M. Q. Khan
Department of Textile Engineering, Faculty of Engineering and Technology, National Textile University Karachi Campus, Karachi, Pakistan

H. Lee
Korea Institute of Industrial Technology, 143, Hanggaul-ro, Sangnok-gu, Ansan-si, Gyeonggi-do, Republic of Korea

Y. Mukai
Department of Chemical Systems Engineering, Nagoya University, Furo-cho, Chikusa-ku, Nagoya 464-8603, Japan

Graphic abstract
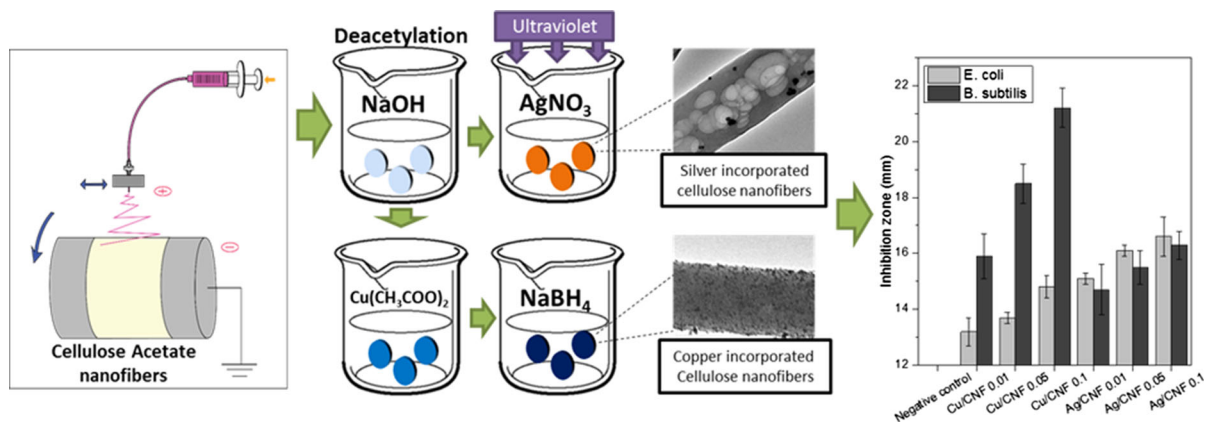
Introduction

Cellulose is a natural material thus considered environmentally friendly in contrast to fossil fuel-based commodity polymers regarding biodegradability and the environmental consequences (Zhu et al. 2016). In consideration of new composite materials with low environmental impact, cellulose is rising as a promising alternative for oil-derived polymers and has attracted much interest in academia, as well as industrial sectors. In recent years, cellulose or cellulosic derivatives have been widely utilized for electrospinning to fabricate nano-sized fibers with multiple functions (Gopiraman et al. 2016). Cellulose nanofibers offer good mechanical properties—approximately 5 MPa in the tensile test (Phan et al. 2019), chemical resistance, and thermal stability (Greish et al. 2010). Cellulose nanofibers have presented great potential in filtration, food packaging, electronic devices, food additives, and medical and cosmetic products (Rezaei et al. 2015).

Pathogenic bacteria are the root of numerous diseases and infections which cause human sickness. To cure those infectious diseases, diverse antibacterial agents have been utilized, including metallic nanoparticles (Kohanski et al. 2010). Silver nanoparticles are considered as a new class of antibacterial agent, with sustainable activity against a wide spectrum of bacteria (Franci et al. 2015); until now no life-threatening risks ensuing from inhalation, ingestion or dermal application of AgNPs have been reported hence AgNPs in suitable doses are considered to be safe for humans (Calderón-Jiménez et al. 2017). For thousands of years, copper has been used as a powerful antibiotic agent and liquid disinfection (Yang et al. 2017). Moreover, copper promotes human cell and tissue regeneration during wound treatment and has been combined with other materials to improve the healing effects (Lokhande et al. 2017). Copper in small doses exhibits negligible cytotoxicity on human cells, yet lethal effects on bacteria (Beyth et al. 2015).

There are several well-reported routes to synthesizing metallic nanoparticles, including chemical, physical, photochemical and biological methods (Iravani et al. 2014). Chemical methods, with three main elements involved metal precursors, reducing agents, and stabilizing agents, can be used to regulate metal nanoparticles in a variety of sizes and shapes with high uniformity and time-saving feature (Zielińska et al. 2009). The physical route has been described as implementing heat generating systems (Dankovich 2014), electric discharge plasma (Lee et al. 2014), and an electric arc discharge (Kawamura et al. 1998) to reduce metal precursor to metal nanoparticles. Recently, biological methods, employing bacteria or substances extracted from plants for silver or copper nanoparticle synthesis, have emerged as an environmentally friendly, economical, and promising route (Iravani 2011; Kuppusamy et al. 2016; Lee et al.

2013). When integrating into medical devices, it is a necessity to eliminate any consequent risk for human health, as well as environments. Therefore, photochemical approaches without the use of additional reagents are regarded as sustainable alternatives for silver nanoparticles syntheses.

The electrospinning method is an effective approach to fabricate ultra-thin fibers with high specific surface area and controllable porosity, hence ideal for applications in tissue engineering scaffolds, wound dressings, and drug delivery (Phan et al. 2018). To conduct electrospinning, the desired polymers are first dissolved in solvent systems, single or co-solvent. A high voltage–power supply with adjustable voltages and a rotary collector to obtain fibers in random orientation are the required apparatus. The former one produces electrical force to overcome the surface tension of the droplet, and an electrified fluid jet is subsequently spun and elongated. While the jet is traveling through the air, the solvent evaporation takes place, and thin fibers accumulate at the collector (Lee et al. 2017; Zhu et al. 2017).

Attempts to incorporate metal nanoparticles into the polymer matrix of nanofibers have made significant progress (Ifuku et al. 2015; Kohsari et al. 2016). Metal nanoparticle-based composite nanofibers demonstrate great advantages to facilitate the uniform distribution and the controllable release of silver or copper at the bacteria contact surfaces (Chen and Peng 2017). For this reason, we opted for silver and copper nanoparticles loaded on cellulosic nanofibers as a functional composite material with antibacterial effects. There have been several scientific articles investigating the synthesis and growth of silver nanoparticles on fibers via the ultraviolet radiation (UV)-induced method (Kozicki et al. 2013; Omrani and Taghavinia 2012; Perera et al. 2013; Rehan et al. 2017). The absorption of silver ions in cellulose was governed by the hydroxyl groups on cellulose nanofibers (Jatoi et al. 2019), and the UV light played the role of reducing agent. The introduction of copper nanoparticles and their antibacterial properties have also been presented on other research papers (Jia et al. 2012; Rubilar et al. 2013). In our study, we successfully coated the silver and copper metals in the nanofibrous cellulosic framework and juxtaposed the UV-facilitating synthesis of AgNPs and the chemical synthesis of CuNPs regarding the metal loading effectiveness on the nanofibrous scaffolds, the metal release properties, and the antibacterial activity against two representative bacteria strains, *E. coli* and *B. subtilis*.

Experimental

Materials

Cellulose acetate (39.8% acetyl weight content, average Mw = 30,000 g mol^{-1}) was purchased from Sigma Aldrich Chemical Co., Ltd (USA). Dimethylformamide (DMF 99.8%), acetone (99.5%), nitric acid (HNO$_3$ 65 wt%), silver nitrate (AgNO$_3$ 99.8%), and copper (II) acetate (Cu(CH$_3$COO)$_2$ 97%) were obtained from Wako Pure Chemical Industries, Ltd. (Japan). All chemicals were used without any additional purification. *Escherichia coli* strain (Hrf 3000) was received from the Coli Genetic Stock (CGSC; Yale Univ., New Haven, CT, USA). *Bacillus subtilis* strain (168) was provided by Dr. Ogasawara, Shinshu University, Japan. The Cell Counting Kit-8 (CCK-8) was purchased from Dojindo Laboratories Japan. The Luria–Bertani broth was purchased in an analytical grade from Nacalai Tesque, INC., Kyoto, Japan. The Petri dishes were supplied by Sansei Medical Co., LTD., Japan.

Fabrication of cellulose nanofibers

Firstly, cellulose acetate was dissolved in the mixture of Acetone/DMF with the weight ratio between two solvents 2/3 to prepare a 20 wt% solution of the polymer. The solution was vigorously agitated for 24 h to ensure all components mixed thoroughly. The electrospinning was set up with a high voltage–power supply (Har-100 * 12, Matsusada Co., Tokyo, Japan), a collector, and a syringe pump. A 20-ml plastic syringe, with a metallic needle affixed to it, was used to contain the prepared solution. The inner diameter of the needle was 1.2 mm, and the distance between the tip of the needle and the collector was adjusted to 18 cm. The syringe pump was set to a flow-rate of 1 ml h^{-1}, and the spinning was performed for 48 h. The parameters were set as voltage of 15 kV, room temperatures, and humidity of approximately 40%.

Once the spinning process was completed, the cellulose acetate nanofibrous sheet was removed from the collector and immersed in sodium hydroxide

solution 0.1 M for 36 h. The deacetylation reaction took place slowly to transform cellulose acetate nanofibers (CANFs) to CNFs. The CNFs were then submerged in dilute nitric acid 0.001 M for 1 h to remove all excessive amount of NaOH and subsequently washed several times with deionized water (DI water). Afterward, the resulted nanofiber mat was cut into round-shaped specimens with a diameter of 12 mm in preparation for further processes.

The synthesis of silver nanoparticles and copper nanoparticles on the surfaces of cellulose nanofibers

For the formation of silver nanoparticles on the surfaces of CNFs, we opted for the UV facilitation method, which was employed by shaking circular cellulose specimens in $AgNO_3$ solutions 0.01, 0.05, and 0.1 M under the radiation of UV light for 24 h, gradually activated the reduction of $AgNO_3$ to AgNPs on the surfaces of the CNFs. Samples were denoted as Ag/CNFs 0.01, 0.05, and 0.1.

To embed CuNPs in the CNFs, rounded cellulosic specimens were immersed in $Cu(CH_3COO)_2$ solutions 0.01, 0.05, and 0.1 M under gentle agitation for 24 h. Those specimens were taken out and dried at room temperature for 48 h. The chemical reduction of copper nanoparticles was implemented by immersing dried specimens in $NaBH_4$ 0.5 M. Resultant samples were indicated as Cu/CNFs 0.01, 0.05, and 0.1.

After the metal nanoparticle incorporation, all specimens were washed with DI water several times and dried in program control oven (AS ONE DOV-600P, MonotaRo Co., Ltd., Japan) for 24 h at 60 °C.

Characterization

Scanning Electron Microscope (SEM, JSM-6010LA, JEOL, Japan) and Transmission Electron Microscopy (TEM, JEOL 2010 Fas TEM, Tokyo, Japan) were employed for morphological study. Fourier Transform Infrared (FT-IR, Prestige-21, Shimadzu Co., Ltd., Japan) was used for chemical compositions. Elemental analysis was studied on X-ray Photoelectron Spectroscopy (XPS, Kratos Axis-Ultra DLD, Kratos Analytical) and Energy Dispersive X-Ray Spectroscopy (SEM–EDS, JSM-6010LA, JEOL, Japan).

Inductively Coupled Plasma-Atomic Emission Spectroscopy (ICP-AES, Shimadzu ICPS-1000 IV, Shimadzu, Kyoto, Japan) was implemented to determine the silver and copper release in solutions and the metal contents of all treated samples. To investigate the silver or copper contents of composite nanofiber samples, samples were first immersed in concentrated HNO_3 solutions, the reactions between silver or copper species and HNO_3 ensued to dissolve all metal nanoparticles to the solutions. The resultant solutions were then sampled and quantified on ICP.

Silver and copper release kinetics and antibacterial assessment assay

The metal release profiles of nanofibrous samples were examined by submerging 0.15 g CNFs containing silver or copper in 50 mL DI water under the gentle shaking condition—100 rpm for 7 days. 2 mL of liquid specimens were extracted after certain periods of time in order to measure the silver or copper release.

The *E. coli* and *B. subtilis* were chosen as subjects of the antibacterial evaluation. The bacteria were cultured in the LB liquid medium for 24 h, at 37 °C in the case of *E. coli* and 30 °C in the case of *B. subtilis*. Subsequently, the cultures were diluted with saline solution to about 10^6 colony forming unit (CFU)/ml, verified by optical density at 600 nm.

In regard to the inhibition zone test, 200 μL bacteria suspension at the density of 10^6 (CFU)/mL was spread on each agar plate; specimens were then gently placed on top of that. After that, agar plates were cultured for 24 h before being evaluated.

For bactericidal efficacy evaluation, 0.01 g of nanofiber webs were soaked in 1 mL LB broth inoculated with bacteria at the concentration of 10^6 (CFU)/ml under mild shaking of 50 rpm for 8 h. Afterward, bacterial broths were sampled, properly diluted, and spread on the agar plates for 24-h culture in order to count the live bacteria cells. The log reduction was calculated as follows:

$$\text{Log Reduction} = \log_{10}(A/B)$$

where A is the number of bacteria colonies counted and calculated on the agar disk after culturing the negative control sample with bacterial broths. B is the number of bacteria colonies counted and calculated on the agar disk after culturing cellulosic samples containing metal with bacteria.

Results and discussion

Morphology and color study of nanofibers

Figure 1a and b show SEM micrographs of electrospun CANFs and CNFs, no significant changes in the morphologies were observed between them. CANFs and CNFs presented the smooth, featureless morphology with mean diameters of 393 ± 98 nm and 411 ± 120 nm, respectively. The cellulosic nanofibers displayed a wide range of diameter distribution. The nanoparticulate formation on the surfaces of the cellulose nanofibers can be observed in Fig. 1c–h. The mean diameters of Ag/CNFs 0.01, 0.05, and 0.1 were 430 ± 153, 440 ± 115, and 456 ± 100 nm, whereas the mean diameters of Cu/CNFs 0.01, 0.05, and 0.1 were 407 ± 73, 428 ± 79, and 506 ± 77, respectively. These composite fibers presented coarser diameters, compared to CANFs and CNFs, due to the swelling on account of the penetration of silver nitrate and copper (II) acetate into the polymer matrix, as well as the newly formed nanoparticles on the fiber scaffold could also affect the nanofiber diameters. The nanoparticles were observed to be well distributed on CNFs.

Ag/CNFs 0.01, 0.05, and 0.1 samples exhibited a range of brown colors, with or without yellow tints, the yellow tints could be spotted in the case of Ag/CNFs 0.1—Fig. 1e*. These colors were ascribed to partly the interactions between silver ions and cellulose, as well as the nanoparticulate formation of silver. Whereas Cu/CNFs presented a range from grey to black colors, the saturated black color belonged to Cu/CNFs 0.1, Fig. 1h*.

TEM images revealed the porous structure of the CANFs which was also reported in Lee et al. (2018). All post-treated CNFs inherently adopted that porous feature. The high porosity of CANFs could be explained by the phase separation occurred in a co-solvent system of DMF and acetone. This phenomenon sometimes happens in a single solvent system but the polymer solution is electrospun in a high humidity environment, in which water plays the role of the second solvent. Fig. S1 illustrates the pore-forming phenomenon in cellulosic nanofibers. In essence, the phase separation occurs due to the intrinsic distinctions between two solvents, which lead to the heterogeneity in polymer density from area to area. After solvents have been removed by the evaporation process, the pores form at lower polymer-density spots.

AgNPs and CuNPs were detected on the surfaces of CNFs after the photo-induced treatment or chemical reduction. The sizes of silver particles were measured from several TEM photographs and the results were charted in Fig. 2c–h. The average sizes of AgNPs were
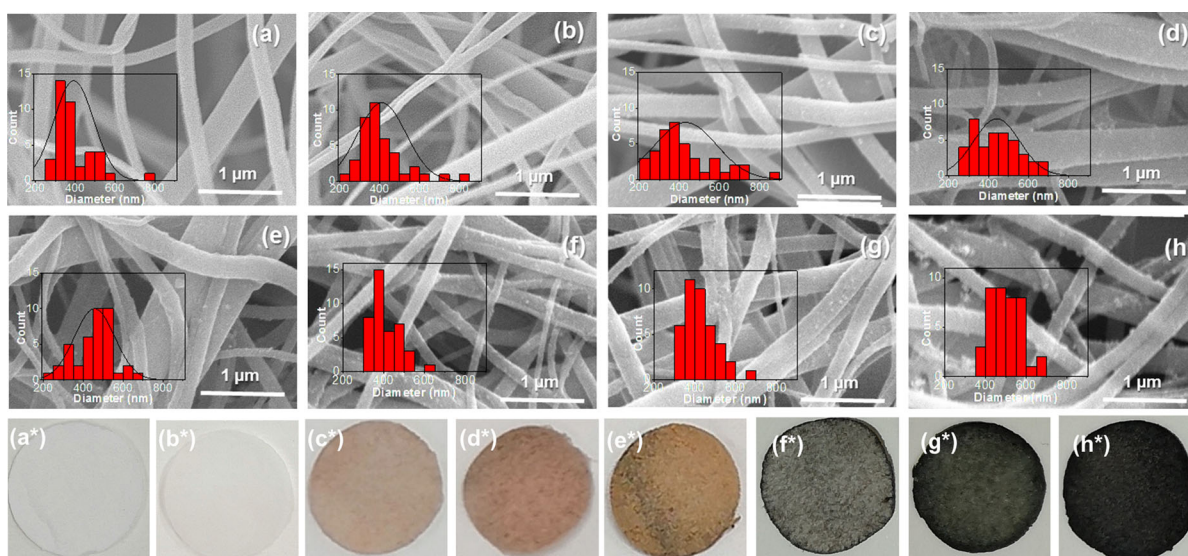

Fig. 1 Morphology and color appearances of **a**, **a*** cellulose acetate nanofibers; **b**, **b*** cellulose nanofibers; Ag/CNFs 0.01 **c**, **c***, 0.05 **d**, **d***, and 0.1 **e**, **e***; Cu/CNFs 0.01 **f**, **f***, 0.05 **g**, **g***, and 0.1 **h**, **h***
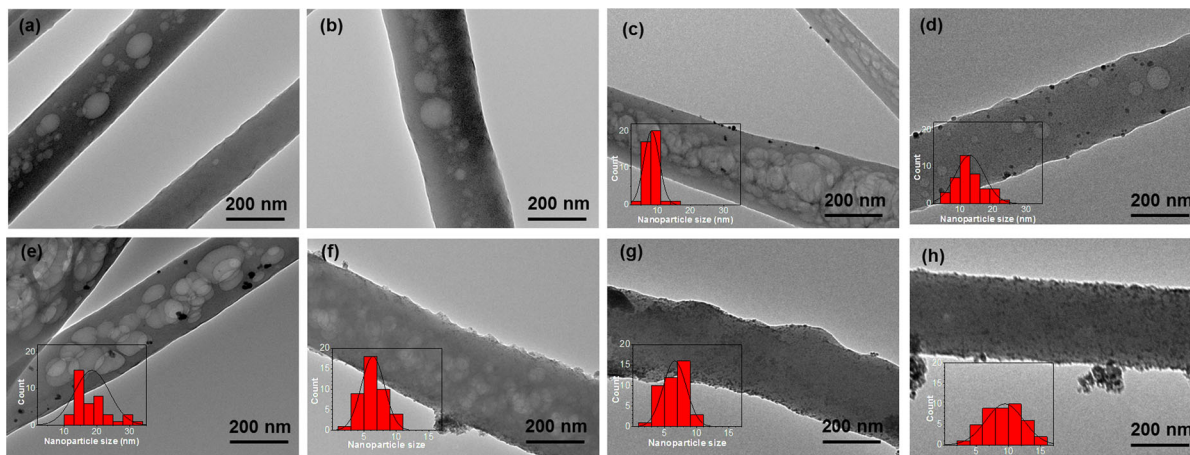
Fig. 2 TEM images of **a** CANFs; **b** CNFs; Ag/CNFs **c** 0.01, **d** 0.05, **e** 0.1; Cu/CNFs **f** 0.01, **g** 0.05, and **h** 0.1

8.2 ± 2.3, 12.9 ± 4.3, and 18.5 ± 5.3 nm respective to treatment in AgNO$_3$ solutions 0.01, 0.05, and 0.1 M under UV radiation. The concentrations of silver salt treating solutions positively influenced the sizes of the AgNPs, the higher the concentrations the larger the particle sizes. In the case of Cu/CNFs samples, the average sizes of CuNPs were 6.5 ± 1.7, 6.7 ± 1.6, and 9.6 ± 2.8, respectively. The CuNPs possessed a more uniform size, and the difference between copper decorated cellulose samples was less significant.

Silver and copper contents

To determine the metal contents in all treated CNFs samples, 0.015 g of metal composite nanofibers was immersed in 50 mL concentrated HNO$_3$ solution for 24 h. ICP was subsequently performed on these solutions to quantify the silver or copper concentrations. The results from the ICP analysis disclosed the metal contents of all composite samples as follows: 0.4 ± 0.2, 3.8 ± 1.0, 6.8 ± 1.7 wt% for Cu/CNFs 0.01, 0.05, and 0.1, Fig. 3I; whereas, Ag/CNFs 0.01, 0.05, and 0.1 possessed silver contents of 6.0 ± 1.4, 8.7 ± 0.8, and 13.6 ± 0.9 wt%, respectively, Fig. 3III. The UV induced synthesis method proved to be effective on loading silver on the nanofiber platforms with the highest silver content of 13.6 wt%, treated in AgNO$_3$ 0.1 M solution. The highest copper loading amount was 6.8 ± 1.7 wt% for Cu/CNFs 0.1. There was a strong correlation between metal contents against the concentrations of treating solutions.

FT-IR spectral study

The FT-IR spectroscopy graphs of CANFs and CNFs reported in Fig. 4, verified the transformation of cellulose acetate into cellulose. The FTIR spectrum of CANFs presented three distinctive peaks at 1750, 1375, and 1230 cm^{-1} which characterized carbonyl C=O stretching, C–CH$_3$ bending, and C–O stretching of acetyl groups in cellulose acetate, respectively (Song et al. 2012). The two peaks at 1750 and 1230 disappeared in the spectroscopy of CNFs, indicating that the acetyl groups were completely removed after the deacetylation reaction with NaOH. The wide-stretching band at 3500–3600, ascribed to the O–H group in CA nanofiber graph, shifted to the new position at 3200–3500 in the case of CNFs nanofiber, and the intensity noticeably increased. Conclusively, the CANFs were fully converted into CNFs.

CNFs showed the typical band at 3200–3500 and peaks of CNFs at 2890, 1640, 1375, 1160, and 1020, attributed to O–H stretching, C–H stretching, H–O–H bending of absorbed water, C–OH bending, C–O antisymmetric bridge stretching, and C–O–C pyranose ring skeletal vibration, respectively (Li et al. 2009). For CNFs treated in AgNO$_3$ under UV excitation, the peak at 820, ascribed to nitrate bending (Oyumi et al. 1985), indicated the presence of nitrate groups in Ag/CNF samples. We surmise that a small amount of AgNO$_3$ penetrated into the CNFs during immersion treatment. The difference in intensity of the 820 cm^{-1} peak must be due to the difference in the quantities of silver nitrate absorbed in the nanofibers; hence, the
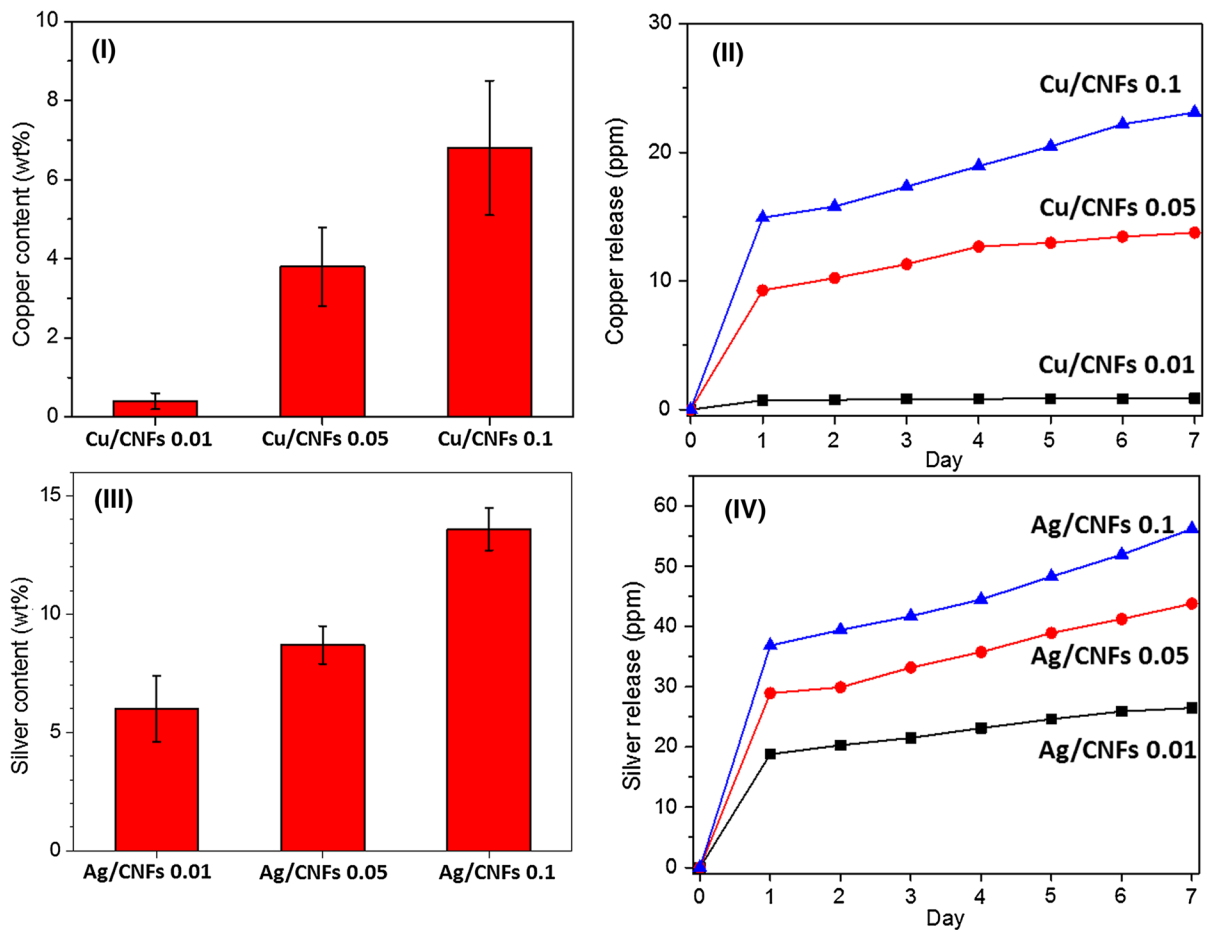
Fig. 3 **I** Copper contents; **II** copper release profiles of Cu/CNFs 0.01, 0.05, and 0.1; **III** Silver contents; and **IV** silver release profiles of Ag/CNFs 0.01, 0.05, and 0.1
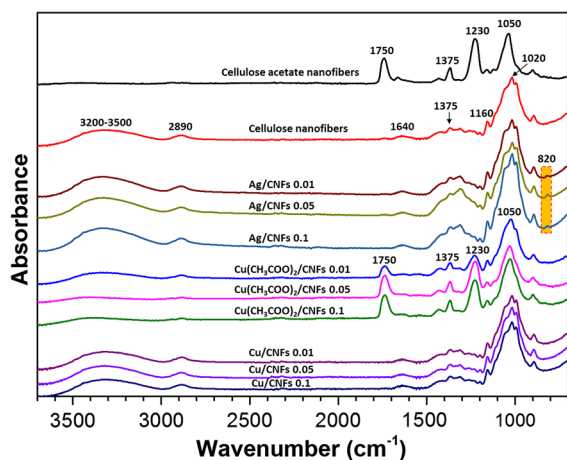

Fig. 4 FT-IR spectra of CANFs, CNFs, Ag/CNFs, copper (II) acetate CNFs, and Cu/CNFs

results suggested that the concentration variation of the treating solutions is one of the factors to alter the silver contents. After immersing CNFs in copper (II) acetate, the acetyl groups were present on CNFs, identified by peaks at 1750, 1375, 1230, and 1050; those peaks were similar to CANFs. After the reduction of copper (II) acetate by sodium borohydride, these peaks disappeared in Cu/CNFs samples, which demonstrated the absolute conversion of copper (II) acetate to zerovalent copper nanoparticles—Cu (0) nanoparticles.

X-ray diffraction study

To identify the nature of metallic nanoparticles, X-ray diffraction patterns were acquired, Fig. 5. CANFs presented two typical diffraction peaks, centered at
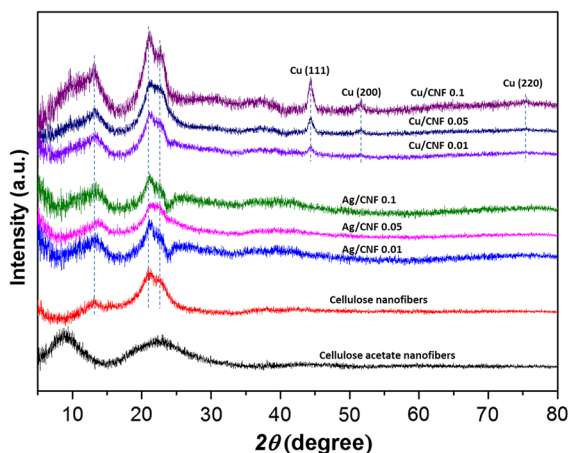
Fig. 5 XRD spectra of CANFs, CNFs, Ag/CNFs, and Cu/CNFs

$2\theta = 9°$ and $22.5°$, which characterized semi-crystallinity of acetylated structure of cellulose acetate (Hong et al. 2013). After the deacetylation reaction, the CNFs displayed peaks which can be ascribed to cellulose II crystallites (French 2014; French and Santiago Cintrón 2013). No Ag/CNF samples showed diffraction peaks for silver, from which we surmised that the nature of silver nanoparticles reduced by UV-excitation was a mixture of zerovalent silver, monovalent silver, and silver salt—AgNO₃; therefore, specific diffraction silver peaks did not appear on silver composite nanofibers. This heterogeneity of AgNPs was thought to cause the difficulty of detecting the silver by XRD. By contrast, CuNPs, reduced by chemical method, could be characterized by 3 typical diffraction peaks at $2\theta = 44°$, $51.5°$, and $75°$, corresponding to 111, 200, and 220 planes of copper nanoparticles (Raffi et al. 2010).

XPS analysis

The presence of metal nanoparticles on CNF samples under UV treatment or chemical synthesis method was further verified by XPS spectra analysis. In Fig. 6I and III, the peaks of O 1s (530.0 eV), C 1s (280.0 eV), and either Ag 3d (from 372.1 to 366.1 eV) or Cu 2p (from 952.3 to 932.4 eV) could be observed in all wide spectra. There are noticeable differences in the intensity of the metal element peaks between samples. Figure 6II, the magnified area at 378–362 eV, identified the silver element, peak positions at 372.1 and 366.1, the gap between two peaks was 6 eV. The

Cu2$p_{1/2}$ and Cu2$p_{3/2}$ signals at 950.6 and 930.6 eV, which were assigned to Cu⁰, demonstrated the reduction of copper (II) acetate to metallic copper. The peak gap was recorded to be about 20 eV (Akgul et al. 2014) (Fig. 6IV).

Metal release kinetics

The release of metal ions over time from the nanoparticles was evaluated to anticipate the bactericidal effects of cellulose composite samples. On the one hand, a speedy release of copper or silver is necessary for the application of wound dressing, thus, the wound is instantaneously cleaned off contaminating organisms; but on the other hand, a slow rate of release ensures a sustainable feature for the membrane in long-term applications. Figure 3II and IV indicate a considerable initial release at the first day for all Cu/CNFs and Ag/CNFs samples, followed by a more gradual discharge of copper or silver into the aqueous environment. The copper release of Cu/CNFs 0.01 sample was stable and almost unchanged during the 7-day course, Fig. 3II. The maximum amounts of silver, discharged at the point of time of 7 days, were 26.47, 43.78, and 56.18 ppm for Ag/CNFs 0.01, 0.05, and 0.1, respectively; whereas they were 0.87, 13.76, and 23.11 for Cu/CNFs 0.01, 0.05, and 0.1. These values accounted for 8.79, 10.04, and 8.25 wt% of the total silver loading amounts on the respective Ag/CNF samples; and 4.5, 8.98, and 8.3 wt% of the total copper loading amounts on respective Cu/CNF samples.

Antibacterial activity against *Escherichia coli* and *Bacillus subtilis*

The antibacterial performance of the composite nanofibers was evaluated against *E. coli* (gram-negative) and *B. subtilis* (gram-positive) bacteria. To confirm that CNFs have no antibacterial activity, CNF specimens were used as the negative control. For all composite samples, disk diffusion test was done in triplicate and the inhibition zones were measured for three specimens. The expansive degrees of halo zones along with standard deviation are illustrated in Fig. 7 and Fig. S4. Cu/CNFs 0.01, 0.05, 0.1, Ag/CNFs 0.01, 0.05, and 0.1 distinctively demonstrated inhibitory zones against bacteria. There was a correlation between the metal release of the silver or copper composite nanofibers and the sizes of the bacterial
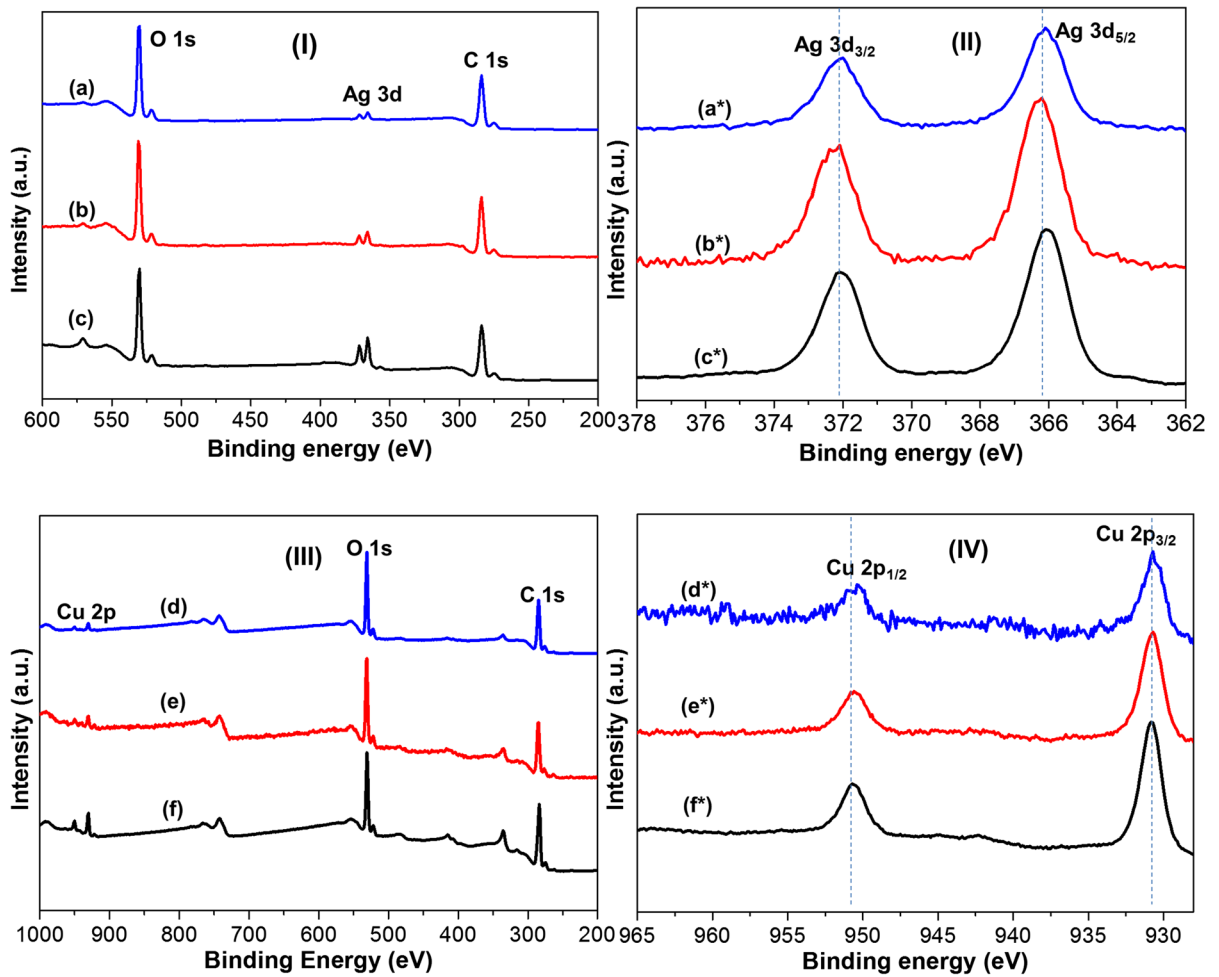
Fig. 6 **I**, **III** XPS wide spectra, and XPS high resolution spectra of the silver region **II** and copper region **IV** for Ag/CNFs 0.01 (a, a*), 0.05 (b, b*), 0.1 (c, c*), and Cu/CNFs 0.01 (d, d*), 0.05 (e, e*), 0.1 (f, f*)
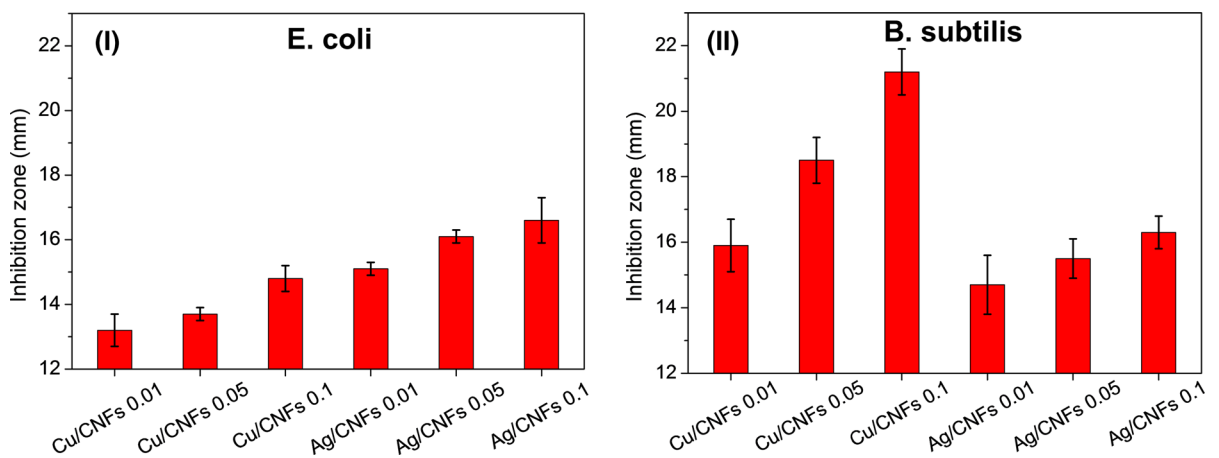

Fig. 7 Mean diameters of inhibition zones with standard deviations against **I** *E. coli* and **II** *B. subtilis* of the composite specimens
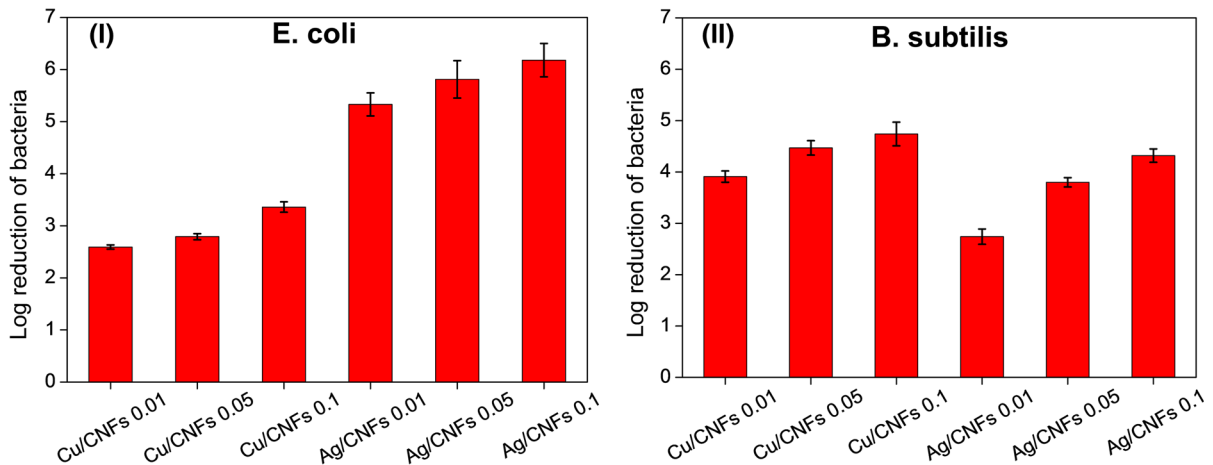
Fig. 8 Bactericidal efficacy of the composite specimens based on agar plate counting method

inhibition zones, to some extent. With the higher metal release amounts, the sizes of inhibition zone were observed to be more expansive. The results indicated that the antibacterial properties of the composite nanofibers were proportionally related to the amounts of the silver or copper releases.

Noticeably, better comparatively expansive inhibition zones against *E. coli* than *B. subtilis* could be observed in the antibacterial assay of Ag/CNF specimens. However, Cu/CNFs exhibited better antibacterial activity against gram-positive bacteria. The inhibition zones of Cu/CNFs were 15.9 ± 0.8, 18.5 ± 0.7, and 21.2 ± 0.7 mm against *B. subtilis*, while only 13.2 ± 0.5, 13.7 ± 0.2, and 14.8 ± 0.4 mm against *E. coli*. The antibacterial results of CuNPs against *B. subtilis* were even higher than those of AgNPs. These results agree well with other scientific reports (Kruk et al. 2015; Yoon et al. 2007).

The bactericidal efficacy against gram-negative *E. coli* and gram-positive *B. subtilis* for the specimen/bacterial broth ratio at 0.01 g/mL was evaluated by agar plate counting as shown in Figs. 8 and S5. The pristine CNF specimens were also prepared as negative controls. Quantitative analyses, which were carried out in triplicate, exhibited an impressive more than 2-log reduction for all composite samples. The disk counting method also demonstrated better bactericidal activity against *E. coli* for silver but copper showed better antibacterial properties against *B. subtilis*. The results were in line with those of disk diffusion tests and other reports (Ruparelia et al. 2008; Yoon et al. 2007).

It was concluded that composites of AgNPs and CNFs synthesized via UV-inducing method exhibited a superior antibacterial activity compared with the composite material Cu/CNFs synthesized via chemical route against gram-negative bacteria—*E. coli*. However, the copper composite samples showed better antibacterial activity against gram-positive bacteria—*B. subtilis*.

Conclusion

The syntheses of silver and copper nanoparticles decorated cellulose nanofibers via two routes, induced through UV excitation or reduced by the chemical reaction, were reported. The study demonstrated that silver and copper nanoparticles loaded on cellulosic scaffolds had potential to exert good antimicrobial properties against *E. coli* and *B. subtilis*. The metal release amounts were observed to be proportionally related to the contents of copper or silver loaded. All metal/cellulose composite nanofibers exhibited good antibacterial activity in terms of inhibition zones and log reduction. Against *E. coli*, silver samples displayed superior antibacterial activity, whereas, against *B. subtilis*, the copper samples demonstrated better.

Compliance with ethical standards

References

Akgul FA, Akgul G, Yildirim N, Unalan HE, Turan R (2014) Influence of thermal annealing on microstructural, morphological, optical properties and surface electronic structure of copper oxide thin films. Mater Chem Phys 147:987–995. https://doi.org/10.1016/j.matchemphys.2014.06.047

Beyth N, Houri-Haddad Y, Domb A, Khan W, Hazan R (2015) Alternative antimicrobial approach: nano-antimicrobial materials. Evid Based Complement Alternat Med 2015:246012. https://doi.org/10.1155/2015/246012

Calderón-Jiménez B, Johnson ME, Montoro Bustos AR, Murphy KE, Winchester MR, Vega Baudrit JR (2017) Silver nanoparticles: technological advances, societal impacts, and metrological challenges. Front Chem 5:6. https://doi.org/10.3389/fchem.2017.00006

Chen L, Peng X (2017) Silver nanoparticle decorated cellulose nanofibrous membrane with good antibacterial ability and high water permeability. Appl Mater Today 9:130–135. https://doi.org/10.1016/j.apmt.2017.06.005

Dankovich TA (2014) Microwave-assisted incorporation of silver nanoparticles in paper for point-of-use water purification. Environ Sci Nano 1:367–378. https://doi.org/10.1039/C4EN00067F

Franci G, Falanga A, Galdiero S, Palomba L, Rai M, Morelli G, Galdiero M (2015) Silver nanoparticles as potential antibacterial agents. Molecules 20:8856

French AD (2014) Idealized powder diffraction patterns for cellulose polymorphs. Cellulose 21:885–896. https://doi.org/10.1007/s10570-013-0030-4

French AD, Santiago Cintrón M (2013) Cellulose polymorphy, crystallite size, and the segal crystallinity index. Cellulose 20:583–588. https://doi.org/10.1007/s10570-012-9833-y

Gopiraman M, Jatoi AW, Hiromichi S, Yamaguchi K, Jeon H-Y, Chung I-M, Ick Soo K (2016) Silver coated anionic cellulose nanofiber composites for an efficient antimicrobial activity. Carbohydr Polym 149:51–59. https://doi.org/10.1016/j.carbpol.2016.04.084

Greish YE, Meetani MA, Al Matroushi EA, Shamsi BA (2010) Effects of thermal and chemical treatments on the structural stability of cellulose acetate nanofibers. Carbohydr Polym 82:569–577. https://doi.org/10.1016/j.carbpol.2010.05.012

Hong C-H, Ki S-J, Jeon J-H, H-l Che, Park I-K, Kee C-D, Oh I-K (2013) Electroactive bio-composite actuators based on cellulose acetate nanofibers with specially chopped polyaniline nanoparticles through electrospinning. Compos Sci Technol 87:135–141. https://doi.org/10.1016/j.compscitech.2013.08.006

Ifuku S et al (2015) Facile preparation of silver nanoparticles immobilized on chitin nanofiber surfaces to endow antifungal activities. Carbohydr Polym 117:813–817. https://doi.org/10.1016/j.carbpol.2014.10.042

Iravani S (2011) Green synthesis of metal nanoparticles using plants. Green Chem 13:2638–2650. https://doi.org/10.1039/C1GC15386B

Iravani S, Korbekandi H, Mirmohammadi SV, Zolfaghari B (2014) Synthesis of silver nanoparticles: chemical, physical and biological methods. Res Pharm Sci 9:385–406

Jatoi AW, Kim IS, Ni QQ (2019) A comparative study on synthesis of AgNPs on cellulose nanofibers by thermal treatment and DMF for antibacterial activities. Mater Sci Eng C 98:1179–1195. https://doi.org/10.1016/j.msec.2019.01.017

Jia B, Mei Y, Cheng L, Zhou J, Zhang L (2012) Preparation of copper nanoparticles coated cellulose films with antibacterial properties through one-step reduction. ACS Appl Mater Interfaces 4:2897–2902. https://doi.org/10.1021/am3007609

Kawamura H, Moritani K, lto Y (1998) Discharge electrolysis in molten chloride: formation of fine silver particles. Plasmas Ions 1:29–36. https://doi.org/10.1016/S1288-3255(99)80004-5

Kohanski MA, Dwyer DJ, Collins JJ (2010) How antibiotics kill bacteria: from targets to networks. Nat Rev Microbiol 8:423–435. https://doi.org/10.1038/nrmicro2333

Kohsari I, Shariatinia Z, Pourmortazavi SM (2016) Antibacterial electrospun chitosan–polyethylene oxide nanocomposite mats containing bioactive silver nanoparticles. Carbohydr Polym 140:287–298. https://doi.org/10.1016/j.carbpol.2015.12.075

Kozicki M et al (2013) Facile and durable antimicrobial finishing of cotton textiles using a silver salt and UV light. Carbohydr Polym 91:115–127. https://doi.org/10.1016/j.carbpol.2012.08.015

Kruk T, Szczepanowicz K, Stefańska J, Socha RP, Warszyński P (2015) Synthesis and antimicrobial activity of monodisperse copper nanoparticles. Colloids Surf B Biointerfaces 128:17–22. https://doi.org/10.1016/j.colsurfb.2015.02.009

Kuppusamy P, Yusoff MM, Maniam GP, Govindan N (2016) Biosynthesis of metallic nanoparticles using plant derivatives and their new avenues in pharmacological applications—an updated report. Saudi Pharm J 24:473–484. https://doi.org/10.1016/j.jsps.2014.11.013

Lee H-J, Song JY, Kim BS (2013) Biological synthesis of copper nanoparticles using Magnolia kobus leaf extract and their antibacterial activity. J Chem Technol Biotechnol 88:1971–1977. https://doi.org/10.1002/jctb.4052

Lee S-W et al (2014) Effect of temperature on the growth of silver nanoparticles using plasmon-mediated method under the irradiation of green LEDs. Materials 7:7781

Lee H, Xu G, Kharaghani D, Nishino M, Song KH, Lee JS, Kim IS (2017) Electrospun tri-layered zein/PVP-GO/zein nanofiber mats for providing biphasic drug release profiles. Int J Pharm 531:101–107. https://doi.org/10.1016/j.ijpharm.2017.08.081

Lee H, Nishino M, Sohn D, Lee JS, Kim IS (2018) Control of the morphology of cellulose acetate nanofibers via electrospinning. Cellulose 25:2829–2837. https://doi.org/10.1007/s10570-018-1744-0

Li J, Zhang L-P, Peng F, Bian J, Yuan T-Q, Xu F, Sun R-C (2009) Microwave-assisted solvent-free acetylation of

cellulose with acetic anhydride in the presence of iodine as a catalyst. Molecules 14:3551

Lokhande AC et al (2017) Novel antibacterial application of photovoltaic Cu2SnS3 (CTS) nanoparticles. RSC Adv 7:33737–33744. https://doi.org/10.1039/C7RA05194H

Omrani AA, Taghavinia N (2012) Photo-induced growth of silver nanoparticles using UV sensitivity of cellulose fibers. Appl Surf Sci 258:2373–2377. https://doi.org/10.1016/j.apsusc.2011.10.038

Oyumi Y, Brill TB, Rheingold AL, Lowe-Ma C (1985) Thermal decomposition of energetic materials. 2. The thermolysis of nitrate and perchlorate salts of the pentaerythrityltetrammonium ion, C(CH2NH3)44 +, by rapid-scan FTIR spectroscopy. The crystal structure of pentaerythrityltetrammonium nitrate ([C(CH2NH3)4](NO3)4). J Phys Chem 89:2309–2315. https://doi.org/10.1021/j100257a033

Perera S, Bhushan B, Bandara R, Rajapakse G, Rajapakse S, Bandara C (2013) Morphological, antimicrobial, durability, and physical properties of untreated and treated textiles using silver-nanoparticles. Colloids Surf A Physicochem Eng Asp 436:975–989. https://doi.org/10.1016/j.colsurfa.2013.08.038

Phan D-N, Lee H, Choi D, Kang C-Y, Im S, Kim I (2018) Fabrication of two polyester nanofiber types containing the biobased monomer isosorbide: poly (ethylene glycol 1,4-cyclohexane dimethylene isosorbide terephthalate) and poly (1,4-cyclohexane dimethylene isosorbide terephthalate). Nanomaterials 8:56

Phan D-N, Lee H, Huang B, Mukai Y, Kim I-S (2019) Fabrication of electrospun chitosan/cellulose nanofibers having adsorption property with enhanced mechanical property. Cellulose 26:1781–1793. https://doi.org/10.1007/s10570-018-2169-5

Raffi M, Mehrwan S, Bhatti TM, Akhter JI, Hameed A, Yawar W, ul Hasan MM (2010) Investigations into the antibacterial behavior of copper nanoparticles against Escherichia coli. Ann Microbiol 60:75–80. https://doi.org/10.1007/s13213-010-0015-6

Rehan M, Barhoum A, Van Assche G, Dufresne A, Gätjen L, Wilken R (2017) Towards multifunctional cellulosic fabric: UV photo-reduction and in situ synthesis of silver nanoparticles into cellulose fabrics. Int J Biol Macromol 98:877–886. https://doi.org/10.1016/j.ijbiomac.2017.02.058

Rezaei A, Nasirpour A, Fathi M (2015) Application of cellulosic nanofibers in food science using electrospinning and its potential risk. Compr Rev Food Sci Food Saf 14:269–284. https://doi.org/10.1111/1541-4337.12128

Rubilar O, Rai M, Tortella G, Diez MC, Seabra AB, Durán N (2013) Biogenic nanoparticles: copper, copper oxides, copper sulphides, complex copper nanostructures and their applications. Biotechnol Lett 35:1365–1375. https://doi.org/10.1007/s10529-013-1239-x

Ruparelia JP, Chatterjee AK, Duttagupta SP, Mukherji S (2008) Strain specificity in antimicrobial activity of silver and copper nanoparticles. Acta Biomater 4:707–716. https://doi.org/10.1016/j.actbio.2007.11.006

Song J, Birbach NL, Hinestroza JP (2012) Deposition of silver nanoparticles on cellulosic fibers via stabilization of carboxymethyl groups. Cellulose 19:411–424. https://doi.org/10.1007/s10570-011-9647-3

Yang J, Xu H, Zhang L, Zhong Y, Sui X, Mao Z (2017) Lasting superhydrophobicity and antibacterial activity of Cu nanoparticles immobilized on the surface of dopamine modified cotton fabrics. Surf Coat Technol 309:149–154. https://doi.org/10.1016/j.surfcoat.2016.11.058

Yoon K-Y, Hoon Byeon J, Park J-H, Hwang J (2007) Susceptibility constants of Escherichia coli and Bacillus subtilis to silver and copper nanoparticles. Sci Total Environ 373:572–575. https://doi.org/10.1016/j.scitotenv.2006.11.007

Zhu Y, Romain C, Williams CK (2016) Sustainable polymers from renewable resources. Nature 540:354. https://doi.org/10.1038/nature21001

Zhu C et al (2017) Enhanced wettability and thermal stability of a novel polyethylene terephthalate-based poly(vinylidene fluoride) nanofiber hybrid membrane for the separator of lithium-ion batteries. ACS Appl Mater Interfaces 9:26400–26406. https://doi.org/10.1021/acsami.7b06303

Zielińska A, Skwarek E, Zaleska A, Gazda M, Hupka J (2009) Preparation of silver nanoparticles with controlled particle size. Procedia Chem 1:1560–1566. https://doi.org/10.1016/j.proche.2009.11.004